Journal of Sound and Vibration (1999) **223**(5), 723–740
Article No. jsvi.1998.2159, available online at http://www.idealibrary.com on IDEAL®

ANALYSIS OF THE NON-LINEAR VIBRATION CHARACTERISTICS OF A BELT-DRIVEN SYSTEM

S. K. KIM

1077 *Ray W. Herrick Laboratories*, *School of Mechanical Engineering*, *Purdue University*, *West Lafayette*, *IN* 47907-1077, *U.S.A.*

AND

J.M. LEE

Department of Mechanical Design and Production Engineering, *Seoul National University*, *Sinrimdong san* 56-1, *Kwanak ku*, *Seoul* 151-741, *Korea*

(*Received* 16 *February* 1998, *and in final form* 9 *December* 1998)

In this paper, a mathematical model for a belt-driven system is proposed to analyze vibration characteristics of driving units having belts, and free and forced vibration analyses are carried out. The mathematical model for a belt-driven system includes belts, pulleys, spindle and bearings. The material properties of each belt and the equivalent stiffnesses supported by pulleys, bearings and a spindle are calculated through experiments. By using Hamilton's principle, four non-linear governing equations and twelve non-linear boundary conditions are derived. To linearize and discretize the non-linear governing equations and boundary conditions, the perturbation and Galerkin methods are used. Also, the free vibration analyses for various parameters of a belt driven system are made, including the tension of a belt, the length of a belt, the material properties of belts, the belt velocity and the pulley mass. Forced vibration analyses of the system are performed, and the dynamic responses for the main parameters are analyzed for a belt driven system.

1. INTRODUCTION

Previous studies [1–7] on belts are mostly confined to obtaining the natural frequencies and modes by free vibration analysis, and are only concerned with the vibration of the belt itself. In the 1980's, the results of studies considering the boundary conditions of both ends of a belt as one-dimensional were presented for the first time, but the forced vibration analysis of a belt-driven system has not been discussed. In an actual belt-driven system, a belt is supported by pulleys, the pulleys suported by driving and driven shafts, and the shafts supported by bearings. In this paper, the one-dimensional boundary condition of a pulley supported system, which was presented by Mote [8, 9], is expanded into two dimensions, and followed by an analysis of vibration transfer through a belt. A mathematical model for the belt, bearing, and pulley in a belt-driven system is also presented, and the free and forced vibrations of an actual belt-driven system

0022–460X/99/250723 + 18 $30.00/0

are analyzed. The material properties of each belt and the equivalent stiffnesses supported by pulleys, bearing and a spindle used in this paper are calculated through experiments.

The contents of this paper are as follows. First, a two dimensional model of support springs of a belt-driven system is presented, Hamilton's principle applied to the model, and finally the non-linear equations of motions of the system are obtained. Second, a numerical analysis program is developed to calculate the natural frequencies and modes of a system. Third, the forced vibrations are analyzed to obtain the dynamic responses for the main parameters of a system, and the effects on the dynamic characteristics of a belt-driven system are considered for the main parameters.

2. THEORETICAL ANALYSIS OF A BELT-DRIVEN SYSTEM

2.1. MODELLING OF A BELT-DRIVEN SYSTEM

The system modelled in this paper is represented by Figure 1. The parameters used for modelling are: E Young's modulus, $\hat{u}$, $\hat{\hat{u}}$ longitudinal displacement of the belts, A cross-sectional area of the belts, $\hat{w}$, $\hat{\hat{w}}$ transverse displacement of the belts, I second moment of area of the belts, θ_L, θ_R rotational displacement of the pulleys, R_0 initial static axial tension of the belts, η_L, η_R x, z direction displacement of the pulleys, R initial axial tension of the belt at speed c, r_L, r_R radius of the pulleys, c initial axial speed of the belts, M_L, M_R mass of the pulleys, m mass per unit length of the belts, J_L, J_R rotational inertia of the pulleys, b thickness of the belts, k_L, k_R support stiffness, L length of the belts, f_j the jth natural frequency, F_{eq} inbalanced load of a motor, $\hat{k}$ equivalent support stiffness.

2.2. DERIVATION OF NON-LINEAR EQUATIONS OF MOTION

The belts are assumed to be in plane motion. In this paper, the supporting stiffness of pulleys is modelled as four linear springs added to two linear springs in the gravitational direction (y direction) in order to expand the model of Mote [8, 9] using only two linear springs in the longitudinal direction (x direction). As the motions of a belt are generally modelled in two dimensions to complete the

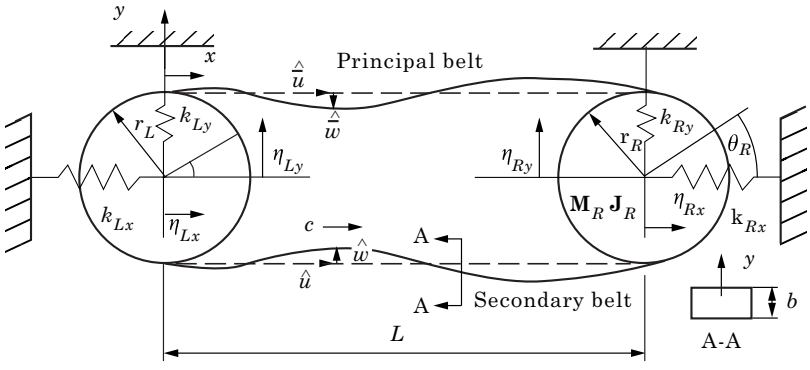

Figure 1. Theoretical model of a belt driven system.

mathematical model of an actual belt-driven system, the motions of pulleys must also be modelled two-dimensionally, in the x and y directions, because the pulleys are supported by the driving and driven shafts, and these shafts are in turn supported by the bearing. The equivalent stiffnesses in the x direction supporting the pulleys are determined by the amplitudes of belt tensions, and those in the y direction by the masses of the pulleys driving and driven shafts, and the boundary conditions. One must consider the non-linearity of the bearing stiffness [10] in the calculation of equivalent stiffnesses supporting the pulleys. Also, the pulleys are modelled as concentrated masses, which exist at both ends, and perform rotational and translational motions (x and z directions). The motion of a belt at the upper and lower ends in contact with the pulleys is confined only to the rotational motion without the translational motion.

Nine assumptions are made in analyzing the proposed model. (1) Each belt is fixed to the pulleys as pin joints. (2) Each belt is a uniform and elastically ranged Euler–Bernoulli beam. (3) The pulleys are connected to the linear springs in the x and y directions. (4) All the values to be analyzed are obtained under the conditions of constant tension and velocity of a belt. (5) There is no slip between the pulleys and belts. (6) All the motions are constrained to the plane. (7) The deflection in the x direction is smaller than that in the y direction. (8) All the variables are only functions of x and t. (9) The relation between the tension R and initial tension R_0 when the feeding velocity is c, is given by

$$R = R_0 + mc^2/[1 + \hat{k}L/(2EA)]. \tag{1}$$

By applying Hamilton's principle to derive the equations of motion, and in Figure 1, expressing the relation between the strain and deflection of a principal belt as equation (2) by the sixth and seventh assumptions above.

$$\hat{\bar{\varepsilon}}_{xx} = \hat{\bar{u}}_x + \hat{\bar{w}}_{,x}^2/2 + R/EA - y\hat{\bar{w}}_{,xx}, \quad \hat{\varepsilon}_{xx} = \hat{u}_{,x} + \hat{w}_{,x}^2/2 + R/EA - y\hat{w}_{,xx}. \tag{2}$$

When small vibrations of a belt occur, the vibration response of the belt can be exactly expressed with linear equations and boundary conditions, but as the amplitude of the belt vibration increases, the effects of the non-linearity also increase. The strain energy of the principal belt is expressed as:

$$U_1 = \tfrac{1}{2}\int_0^L \int_A E\hat{\bar{\varepsilon}}_{xx}^2 \, \mathrm{d}A \, \mathrm{d}x. \tag{3}$$

Using the eighth assumption, equation (2) is inserted into equation (3) to produce the potential energy of the principal belt.

$$U_1 = \tfrac{1}{2}\int_0^L \left(EA\hat{\bar{u}}_{,x}^2 + EA\hat{\bar{u}}_{,x}\hat{\bar{w}}_{,x}^2 + \frac{EA\hat{\bar{w}}_{,x}^4}{4} + \frac{R^4}{EA} + EI\hat{\bar{w}}_{,xx}^2 + 2R\hat{\bar{u}}_{,x} + R\hat{\bar{w}}_{,x}^2 \right) \mathrm{d}x. \tag{4}$$

By using equation (4), the strain energy of the secodary belt is obtained as:

$$U_2 = \tfrac{1}{2}\int_0^L \left(EA\hat{u}_{,x}^2 + EA\hat{u}_{,x}\hat{w}_{,x}^2 + \frac{EA\hat{w}_{,x}^4}{4} + \frac{R^4}{EA} + EI\hat{w}_{,xx}^2 + 2R\hat{u}_{,x} + R\hat{w}_{,x}^2 \right) \mathrm{d}x. \tag{5}$$

The potential energy which is saved by the supporting pulley stiffnesses is given by:

$$U_3 = \tfrac{1}{2}k_{Lx}\left(\eta_{Lx} + \frac{2R}{k_{Lx}}\right)^2 + \tfrac{1}{2}k_{Rx}\left(\eta_{Lx} - \frac{2R}{k_{Rx}}\right)^2 + \tfrac{1}{2}k_{Ly}\eta_{Ly}^2 + \tfrac{1}{2}k_{Ry}\eta_{Ry}^2. \tag{6}$$

The total potential energy of the system is expressed as

$$U = U_1 + U_2 + U_3. \tag{7}$$

The kinetic energy of a belt-driven system assuming plane motion is:

$$\begin{aligned} T = {} & \tfrac{1}{2}\int_0^L m\left[\left(c + \frac{\mathrm{d}\hat{u}}{\mathrm{d}t}\right)^2 + \left(\frac{\mathrm{d}\hat{w}}{\mathrm{d}t}\right)^2\right]\mathrm{d}x + \tfrac{1}{2}\int_0^L m\left[\left(-c + \frac{\mathrm{d}\hat{\bar{u}}}{\mathrm{d}t}\right)^2 + \left(\frac{\mathrm{d}\hat{\bar{w}}}{\mathrm{d}t}\right)^2\right]\mathrm{d}x \\ & + \tfrac{1}{2}\hat{J}\left(\frac{\mathrm{d}\theta_L}{\mathrm{d}t} + \frac{c}{r_L}\right)^2 + \tfrac{1}{2}\hat{J}_R\left(\frac{\mathrm{d}\theta_R}{\mathrm{d}t} + \frac{c}{r_R}\right)^2 \\ & + \tfrac{1}{2}\hat{M}_L\left(\frac{\mathrm{d}\eta_{Lx}^2}{\mathrm{d}t} + \frac{\mathrm{d}\eta_{Ly}^2}{\mathrm{d}t}\right) + \tfrac{1}{2}\hat{M}_R\left(\frac{\mathrm{d}\eta_{Lx}^2}{\mathrm{d}t} + \frac{\mathrm{d}\eta_{Ly}^2}{\mathrm{d}t}\right). \end{aligned} \tag{8}$$

In equation (8), the first and the second terms are the kinetic energy of the belt, and the remaining terms are the rotational and translational kinetic energies of the pulleys. The sum of the work generated by the dynamic load of the motor system, and the constant moments $\hat{M}\hat{M}_R$, $\hat{M}\hat{M}_L$ at both ends of the belt is:

$$\begin{aligned} W = {} & f_x\eta_{Lx} + f_y\eta_{Ly} + \hat{M}\hat{M}_R\hat{w}_{,x}(L, t) - \hat{M}\hat{M}_L\hat{w}_{,x}(0, t) \\ & - \hat{M}\hat{M}_R\hat{\bar{w}}_{,x}(L, t) + \hat{M}\hat{M}_L\hat{\bar{w}}_{,x}(0, t). \end{aligned} \tag{9}$$

In order to calculate the potential energy for the pulleys and supporting stiffness, one must impose conditions of geometric compatibility at both ends of the belt for the rotational and translational motions of pulleys. The geometric compatibility for the rotational and translational motions of pulleys is:

$$\begin{aligned} \theta_L(t) &= [\hat{u}(0, t) - \hat{\bar{u}}(0, t)]/2r_L, \quad \theta_R(t) = [\hat{u}(L, t) - \hat{\bar{u}}(L, t)]/2r_R, \\ \eta_{Lx} &= [\hat{u}(0, t) + \hat{\bar{u}}(0, t)]/2, \quad \eta_{Rx} = [\hat{u}(L, t) + \hat{\bar{u}}(L, t)]/2, \\ \eta_{Ly} &= [\hat{w}(0, t) + \hat{\bar{w}}(0, t)]/2, \quad \eta_{Ry} = [\hat{w}(L, t) + \hat{\bar{w}}(L, t)]/2. \end{aligned} \tag{10}$$

By using Hamilton's principle, one can derive equation (11) (a full expansion of equation (11) is given in the Appendix) by combining the above equations.

$$\delta H = \int_{t_1}^{t_2} (\delta T - \delta U + \delta W)\,\mathrm{d}t. \tag{11}$$

The next procedure is the non-dimensionalization of the governing equations and boundary conditions from equation (11) so that one can derive the four dimensionless governing equations ((12)–(15)) and twelve boundary conditions (equations (16)–(25)).

For $0 \leqslant \xi \leqslant 1$, $\tau > 0$

$$\ddot{u} - 2s\dot{u}' - \Phi u'' - \gamma w'' w' = 0, \quad \ddot{\bar{u}} - 2s\dot{\bar{u}}' - \Phi \bar{u}'' - \gamma \bar{w}'' \bar{w}' = 0, \tag{12, 13}$$

$$\ddot{w} + 2s\dot{w}' - \Psi w'' + w'''' - \gamma(u'' w' + u' w'') - 1{\cdot}5\alpha w'^2 w'' = 0, \tag{14}$$

$$\ddot{\bar{w}} + 2s\dot{\bar{w}}' - \Psi \bar{w}'' + \bar{w}'''' - \gamma(\bar{u}'' \bar{w}' + \bar{u}' \bar{w}'') - 1{\cdot}5\alpha \bar{w}'^2 \bar{w}'' = 0, \tag{15}$$

$$(J_L/2\rho_L^2)(\ddot{u}(0, t) - \ddot{\bar{u}}(0, \tau)) - \beta(u'(0, \tau) - \bar{u}'(0, \tau))$$

$$-(\gamma/2)(w'^2(0, \tau) - \bar{w}'^2(0, \tau)) = 0, \tag{16}$$

$$(M_L/2)(\ddot{u}(0, t) + \ddot{\bar{u}}(0, \tau)) + (k_{Lx}/2)(u(0, \tau) + \bar{u}(0, \tau))$$

$$-\beta(u'(0, \tau) + \bar{u}'(0, \tau)) - (\gamma/2)(w'^2(0, \tau) + \bar{w}'^2(0, \tau)) = \bar{f}_x, \tag{17}$$

$$(J_R/2\rho_R^2)(\ddot{u}(1, \tau) - \ddot{\bar{u}}(1, \tau)) + \beta(u'(1, \tau) - \bar{u}'(1, \tau))$$

$$+(\gamma/2)(w'^2(1, \tau) - \bar{w}'^2(1, \tau)) = 0, \tag{18}$$

$$(M_R/2)(\ddot{u}(1, t) + \ddot{\bar{u}}(1, \tau)) + (k_{Rx}/2)(u(1, \tau) + \bar{u}(1, \tau))$$

$$+\beta(u'(1, \tau) + \bar{u}'(1, \tau)) + (\gamma/2)(w'^2(1, \tau) + \bar{w}'^2(1, \tau)) = 0, \tag{19}$$

$$(w'''(0, \tau) - \bar{w}'''(0, \tau)) - \gamma(u'(0, \tau) w'(0, \tau) - \bar{u}'(0, \tau)\bar{w}'(0, \tau))$$

$$-(\alpha/2)(w'^3(0, \tau) - \bar{w}'^3(0, \tau)) - R_n(w'(0, \tau) - \bar{w}'(0\,\tau)) = 0, \tag{20}$$

$$(M_L/2)(\ddot{w}(0, \tau) + \ddot{\bar{w}}(0, \tau)) + (k_{Ly}/2)(w(0, \tau) + \bar{w}(0, \tau))$$
$$- \gamma(u'(0, \tau) w'(0, \tau) + \bar{u}'(0, \tau)\bar{w}'(0, \tau)) - (\alpha/2)(w'^3(0, \tau) + \bar{w}'^3(0, \tau))$$
$$+ (w'''(0, \tau) + \bar{w}'''(0, \tau)) - R_n(w'(0, \tau) + \bar{w}'(0, \tau)) = \bar{f}_y, \tag{21}$$

$$(w'''(1, \tau) - \bar{w}'''(1, \tau)) - \gamma(u'(1, \tau) w'(1, \tau) - \bar{u}'(1, \tau)\bar{w}'(1, \tau))$$
$$- (\alpha/2)(w'^3(1, \tau) - \bar{w}'^3(1, \tau)) - R_n(w'(1, \tau) - \bar{w}'(1, \tau)) = 0, \tag{22}$$

where

$$\dot{u} = \partial u/\partial t, \quad u' = \partial u/\partial x, \quad \dot{w} - \partial w/\partial t, \quad w' = \partial w/\partial x$$

$$(M_R/2)(\ddot{w}(1,\tau)+\ddot{\bar{w}}(1,\tau))+(k_{Ry}/2)(w(1,\tau)+\bar{w}(1,\tau))$$
$$-(w'''(1,\tau)+\bar{w}'''(1,\tau))+\gamma(u'(1,\tau)w'(1,\tau)+\bar{u}'(1,\tau)\bar{w}'(1,\tau))$$
$$+(\alpha/2)(w'^3(1,\tau)+\bar{w}'^3(1,\tau))+R_n(w'(1,\tau)+\bar{w}'(1,\tau))=0, \quad (23)$$

$$w''(0,\tau)=\bar{w}''(0,\tau)=0, \quad w''(1,\tau)=\bar{w}''(1,\tau)=0 \quad (24,25)$$

2.3. LINEARIZATION

Non-linear terms exist in the derived governing equations and boundary conditions (12)–(25) for the mathematical analysis of a belt-driven system. These non-linear governing equations and boundary conditions are linearized by applying the perturbation method from reference [11], so that the non-linear variables u, $\bar{u}$, w, $\bar{w}$ become the summation of two linear variables.

$$u(\xi,\tau)=u^*(\xi)+u(\xi,\tau), \quad \bar{u}(\xi,\tau)=\bar{u}^*(\xi)+\bar{u}(\xi,\tau),$$
$$w(\xi,\tau)=w^*(\xi)+w(\xi,\tau), \quad \bar{w}(\xi,\tau)=\bar{w}^*(\xi)+\bar{w}(\xi,\tau). \quad (26)$$

By inserting equation (26) into equations (12)–(25) and removing non-linear terms, the linear governing equations and boundary conditions can be derived (see the Appendix).

2.4. DISCRETIZATION

Generally, the exact solution of the linear governing equations and boundary conditions cannot be calculated, so one discretizes them by using the weak form of Galerkin [12]. Equation (27) expresses the governing equations and boundary conditions as the operator, and equation (28) produces the residual terms.

$$L_m[u,w,\bar{u},\bar{w}]=0, \quad m=1\text{–}4, \quad B_n[u,w,\bar{u},\bar{w}]=0, \quad n=1\text{–}8, \quad (27)$$

$$e_{dm}=L_m[u,w,\bar{u},\bar{w}]=0, \quad m=1\text{–}4, \quad e_{bn}=B_n[u,w,\bar{u},\bar{w}]=0, \quad n=1\text{–}8, \quad (28)$$

Separation of variables is performed on the variables u, $\bar{u}$, w, $\bar{w}$, to give

$$u(\xi,\tau)=\sum_{i=1}^{N}U_i(\xi)p_i(\tau), \quad \bar{u}(\xi,\tau)=\sum_{i=1}^{N}\bar{U}_i(\xi)\bar{p}_i(\tau),$$
$$w(\xi,\tau)=\sum_{i=1}^{N}W_i(\xi)q_i(\tau), \quad \bar{w}(\xi,\tau)=\sum_{i=1}^{N}\bar{W}_i(\xi)\bar{q}_i(\tau). \quad (29)$$

Here, $p_i(\tau)$, $q_i(\tau)$, $\bar{p}_i(\tau)$, $\bar{q}_i(\tau)$ are the general co-ordinates. The assumption for the functions $U_i(\xi)$, $W_i(\xi)$, $\bar{U}_i(\xi)$, $\bar{W}_i(\xi)$ is expressed by:

$$U_i(\xi),\ \bar{U}_i(\xi),\ \text{admissible function}; \quad W_i(\xi),\ \bar{W}_i(\xi),\ \text{comparison function}. \quad (30)$$

In particular, the assumption made for the function $U_i(\xi)$ determines the admissible function of a beam at both free ends, because both ends of a belt behave freely in the x direction, and the assumption for $W_i(\xi)$ determines the

comparison function, because both ends of a belt behave freely in the gravitational direction (y direction), and the moments become zero at both ends of a belt. The discretized weak form of a belt-driven system by the Galerkin method can be stated as:

$$\langle e_{d1},\, u_j(\xi)\rangle + \sum_{n=1}^{4}(e_{bn}U_{bj}) = 0, \quad \langle e_{d2},\, \bar{U}_j(\xi)\rangle + \sum_{n=1}^{4}(e_{bn}\bar{U}_{bj}) = 0,$$

$$\langle e_{d3},\, w_j(\xi)\rangle + \sum_{n=5}^{8}(e_{bn}U_{bj}) = 0, \quad \langle e_{d4},\, \bar{w}_j(\xi)\rangle + \sum_{n=5}^{8}(e_{bn}\bar{W}_{bj}) = 0. \tag{31}$$

In equation (31), $\langle\ \rangle$ is the inner product without the weighting at $0<\xi<1$ and U_b and $\bar{U}_b$ are the values of $U_j(\xi)$, $\bar{U}_j(\xi)$ to be calculated at $\xi = 0$ and $\xi = 1$. The assumed functions are inserted into equation (31), so that the final equation of motion becomes

$$[\mathbf{M}]\{\ddot{\mathbf{y}}(\tau)\} + [\mathbf{G}]\{\dot{\mathbf{y}}(\tau)\} + [\mathbf{K}]\{\mathbf{y}(\tau)\} = \{\mathbf{F}\}. \tag{32}$$

Here, the shapes and elements of each matrix are:

$$[\mathbf{M}] = \begin{bmatrix} M_{11} & M_{12} & 0 & 0 \\ M_{21} & M_{22} & 0 & 0 \\ 0 & 0 & M_{33} & M_{34} \\ 0 & 0 & M_{43} & M_{44} \end{bmatrix}, \quad [\mathbf{G}] = \begin{bmatrix} G_{11} & 0 & 0 & 0 \\ 0 & G_{22} & 0 & 0 \\ 0 & 0 & G_{33} & 0 \\ 0 & 0 & 0 & G_{44} \end{bmatrix}, \tag{33, 34}$$

$$[\mathbf{K}] = \begin{bmatrix} K_{11} & K_{12} & K_{13} & 0 \\ K_{21} & K_{22} & 0 & K_{24} \\ K_{31} & 0 & K_{33} & K_{34} \\ 0 & K_{42} & K_{43} & K_{44} \end{bmatrix}, \quad \{\mathbf{y}\} = \begin{Bmatrix} p \\ \bar{p} \\ q \\ \bar{q} \end{Bmatrix}, \quad \{\mathbf{F}\} = \begin{Bmatrix} (\bar{f}_x/2)\times U_j(0) \\ (\bar{f}_x/2)\times \bar{U}_j(0) \\ (\bar{f}_y/2)\times W_j(0) \\ (\bar{f}_y/2)\times \bar{W}_j(0) \end{Bmatrix}. \tag{35–37}$$

3. NUMERICAL ANALYSIS OF A BELT-DRIVEN SYSTEM

After development of the program of numerical analysis for the equations of motions of a belt-driven system using the previously derived equations, some results of the numerical analysis are reported. First, the free vibration analysis of a belt-driven system, was performed to obtain the natural frequencies and modes. Second, the forced vibration analysis was performed by applying an external load in order to calculate the dynamic responses of the main parameters representing the characteristics of the system. All data to be used for these analyses, which were the shapes and material properties of belts, the shapes and supporting stiffnesses of pulleys, and so on, were obtained through the precision dynamic power transfer system in the Institute of Advanced Machinery and Design of Seoul National University as shown in Figure 2. All data values are listed in Tables 1 and 2. Generally, the shaft is supported by the bearing, and the following non-linear experimental equation (see reference [10]) was used to

calculate the equivalent stiffness of a bearing.

$$\text{Stiff} = \mathrm{d}F_r/\mathrm{d}\delta_r = n(1/\xi)ZK\delta_r^{n-1}\cos\alpha, \tag{38}$$

where Z is number of balls, δ_r the radial displacement, n is a constant (1·5 in the case of a ball bearing), α the contact angle (for the bearing used 30°), K the load–deflection constant (130 000 in the case of a ball bearing), ξ is a constant (4·37 in the case of a ball bearing), F_r is the radial load.

The stiffness of a bearing is related not only to the material property of a bearing, but also to the displacement and external load. Hence the external load on the bearing was calculated and the equivalent stiffness was predicted.

3.1. ANALYSES OF FREE VIBRATION

The free vibration analysis of the system through a written program to calculate eigenvalues of the non-symmetric matrix was performed, and Table 3 shows the natural frequencies of each belt. From the results of the analysis, similar values for each pair of natural frequencies were obtained. It means that these results are in good agreement with those presented by Mote even though the support springs of the pulleys were expanded from one dimension (x direction) to two dimensions (x and y directions). These phenomena can be attributed to the effects of the boundary condition not having been considered in the previous studies, namely, the longitudinal displacements u and $\bar{u}$, and the transverse displacements w and $\bar{w}$ that characterize the pulley rotation and translation in each mode. The rotation of the pulleys is determined by the differences between u and $\bar{u}$ at the boundaries, and the translations of the pulleys are determined by the sums of u and $\bar{u}$, and w and $\bar{w}$ at the boundaries as can be seen in equation (10). It is clear that the longitudinal motions u and $\bar{u}$, and the transverse motions w and $\bar{w}$ oscillate the pulleys, and thus couple the motions of the belts as in the results of Mote [9]. As the difference of a pair of natural frequencies becomes smaller, the effect of coupling decreases [9]. Figures 3, 4 and 5 show the first, second and third mode shapes through using the poly-flex belt, and calculation conditions for the analysis are presented in Tables 1 and 2.

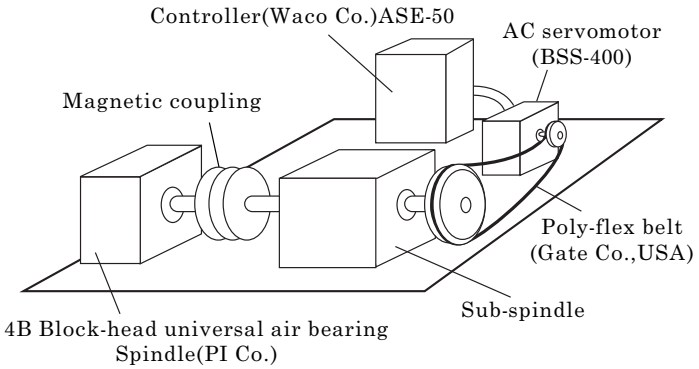

Figure 2. Schematic diagram of precision dynamic drive system.

TABLE 1
Characteristics of belts

Items	Belt type		
	Poly-flex	Timing belt	V-belt
Young's modulus (N/m^2)	1·5433E9	1·350E9	7·4511E8
Width (mm)	4·25	13·0	9·3
Thickness (mm)	5·0	4·0	8·5
Length (mm)	400·0	400·0	400·0
Initial tension (N)	300·0	300·0	300·0

The results are as follows. Firstly, from the free vibration analyses of the system for various belt velocities, as the belt velocity increases, the natural frequencies decrease more or less. Secondly, from the analyses for the various belt lengths, the natural frequencies greatly decrease as the length of a belt becomes longer. Thirdly, from the analyses for various belt tensions, the natural frequencies increase hugely as the belt tension increases. Fourthly, as the elastic modulus of a belt increases, the natural frequencies increase. Finally, one observes that as the pulley mass is increased gradually, the natural frequencies change very little. The increase in pulley mass has little effect on the natural frequencies because the supporting stiffness of a pulley by the bearing is huge. The tension, the elastic modulus and the length of a belt have the main effects on the natural frequencies. Tables 4 and 5 show the results of free vibration analyses for the various parameters of the belt-driven system.

3.2. ANALYSES OF FORCED VIBRATION

In equation (32), the right term was defined as the external load resulting from the dynamic load by the geometric eccentricity of a motor system. One assumed that the inbalanced dynamic load was a sinusoidal function. In order to analyse the forced vibration, the inbalanced dynamic load was inserted in the x and z directions into the external load of equation (32). The dynamic load in the x

TABLE 2
Characteristics of pulleys

Pulley items (steel)	Values
Width (mm)	13·5
Radius of left pulley (mm)	25·0
Radius of right pulley (mm)	50·0
Mass density (kg/m^3)	7·8E3
x direction support stiffness of left pulley (N/m)	7·91E8
x direction support stiffness of right pulley (N/m)	9·59E8
z direction support stiffness of left pulley (N/m)	1·21E7
y direction support stiffness of right pulley (N/m)	5·96E7

TABLE 3
Results of modal analysis

Mode no.	Natural frequency (Hz)		
	Poly-flex	Timing belt	V-belt
1	13·66	11·05	14·26
2	20·44	13·76	25·26
3	20·57	13·93	26·13
4	35·43	25·88	43·32
5	40·36	29·47	47·47
6	51·43	40·55	61·54
7	51·93	40·98	62·14
8	69·98	59·72	81·52
9	76·33	64·22	95·24
10	89·31	79·47	117·21
11	90·31	80·14	117·43

direction was defined as the sine function, and that in the y direction as the cosine function. To calculate the dynamic displacements for the dynamic load, the impedance method was applied to the program of forced vibration analysis, and the data used in the forced vibration analysis are presented in Table 6.

Table 7 and Figure 6 show the results of dynamic analyses of a belt-driven system using the timing belt and a poly-flex belt, and the calculation conditions

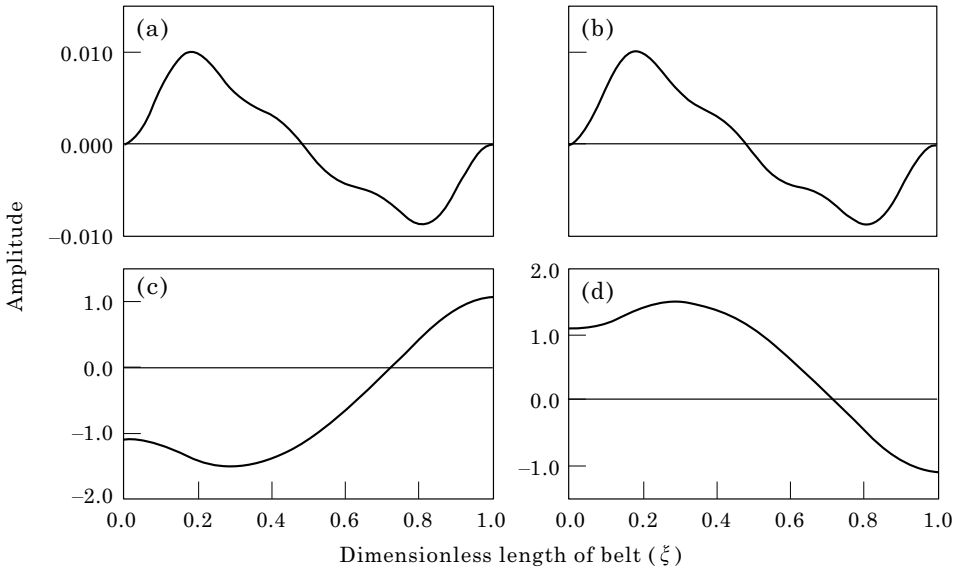

Figure 3. First mode shape of poly-flex belts (f_1 = 13·66 Hz): (a) x directional mode shape of the primary belt; (b) x directional mode shape of the secondary belt; (c) y directional mode shape of the primary belt; (d) y directional mode shape of the secondary belt. The properties of the belt and the support stiffnesses are listed in Tables 1 and 2.

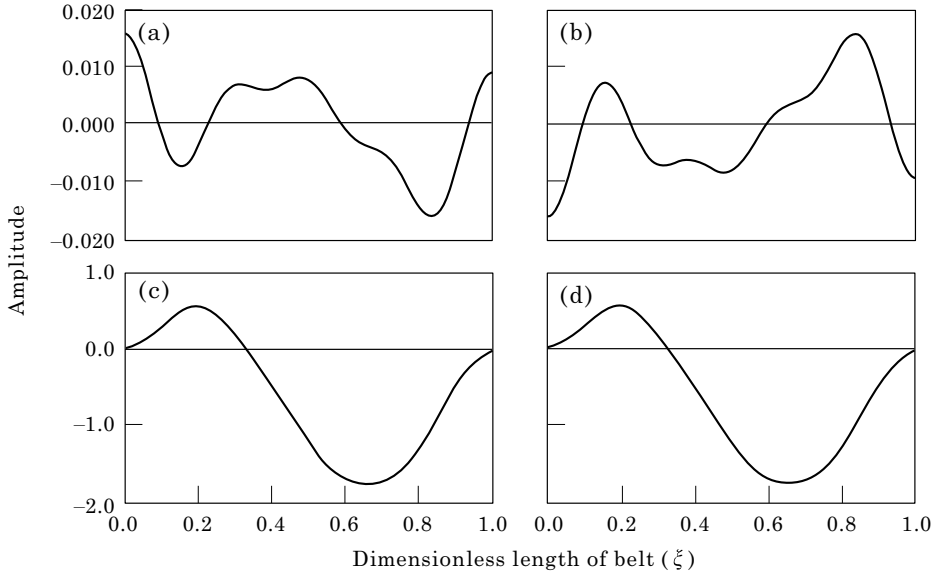

Figure 4. Second mode shape of poly-flex belts ($f_2 = 20{\cdot}44$ Hz): (a) x directional mode shape of the primary belt; (b) x directional mode shape of the secondary belt; (c) y directional mode shape of the primary belt; (d) y directional mode shape of the secondary belt. The properties of the belt and the support stiffnesses are listed in Tables 1 and 2.

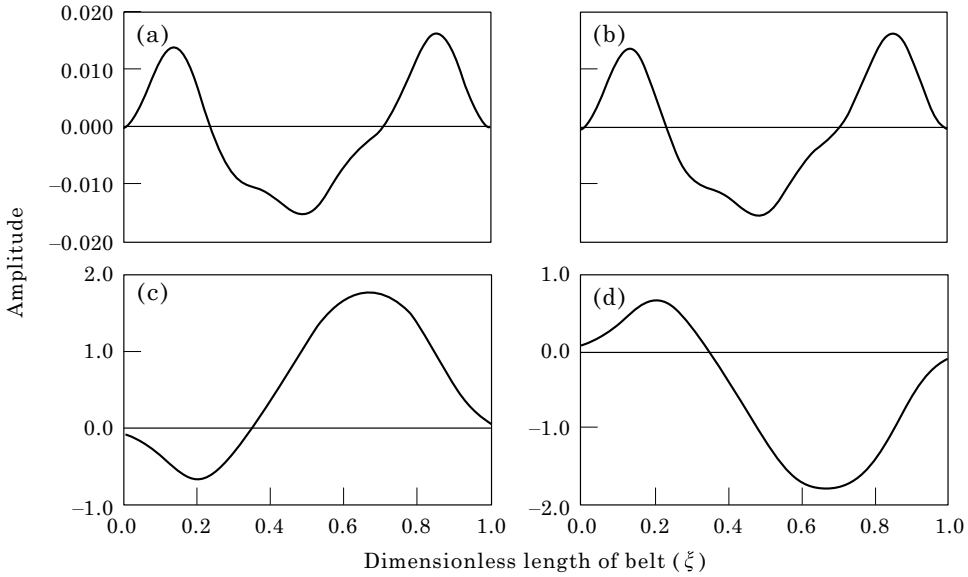

Figure 5. Third mode shape of poly-flex belts ($f_3 = 20{\cdot}57$ Hz): (a) x directional mode shape of the primary belt; (b) x directional mode shape of the secondary belt; (c) y directional mode shape of the primary belt; (d) y directional mode shape of the secondary belt. The properties of the belt and the support stiffnesses are listed in Tables 1 and 2.

TABLE 4

Analysis of free vibrations of systems for the various belt tensions

	Tension (N)			
Mode no.	200·0	300·0	600·0	1000·0
1	10·79	13·66	19·24	24·50
2	14·41	20·44	29·44	36·73
3	14·59	20·57	29·58	36·89
4	26·59	35·43	49·94	62·67
5	30·29	40·36	58·42	74·20
6	40·99	51·43	70·72	88·74
7	41·45	51·93	71·46	89·52
8	59·36	69·98	91·99	114·69
9	64·21	76·33	101·52	125·01
10	78·35	89·31	114·78	126·19
11	79·12	90·31	115·63	138·57

for the analyses are presented in Tables 1, 2 and 6. The displacements were calculated in the x and y directions of the right pulley, and at the excited position, namely the left pulley. The results of the dynamic analysis are as follows. Firstly, the dynamic displacements in the x direction using a timing belt are smaller than those using a poly-flex belt at the excited position. It means that the total stiffness of a system using the timing belt is larger than that of a system using the poly-flex under the same supporting pulley stiffness. Secondly, the dynamic displacements in the x direction of the right pulley using the timing belt are smaller than those using the poly-flex belt, but the dynamic displacements in the y direction of the right pulley have contrary results.

TABLE 5

Analysis of free vibrations of systems for the various belt elastic moduli

	glastic moduli (N/m^2)			
mode no.	1·54E9	5·40E9	7·72E9	1·54E10
1	13·66	25·08	29·80	41·97
2	20·44	37·53	44·18	61·73
3	20·57	37·70	44·36	61·98
4	35·43	64·09	75·76	106·17
5	40·36	75·92	89·99	126·31
6	51·43	90·73	107·27	138·56
7	51·93	91·54	108·13	150·23
8	69·98	117·58	138·53	151·33
9	76·33	128·87	138·99	194·37
10	89·31	138·57	151·80	211·82
11	90·31	145·49	171·49	239·12

TABLE 6
Data to be used in dynamic analysis

Items	Data values
$f_x = f_y = me\omega^2$ (N)	4·1
Tension R (N)	300·0
Time step	5000
Δt (s)	6·28E-7

Another analysis of forced vibration was performed using the poly-flex belt for the various excited forces, and the analytical methods were: belt tension was 300 N, and the excited frequency was 378·0 rad/s (3600 r.p.m.). Table 8 shows the results of the analysis, and as the external excited forces increase, both displacements in the x and y directions of the pulleys increase.

4. CONCLUSIONS

In this paper, a two-dimensional analytical model of support springs by pulleys has been presented, to expand the model by Mote, in order to perform the exact modelling of a belt-driven system. The supporting stiffnesses in two dimensions of pulleys to be considered in the proposed model for an actual belt-driven system was calculated, and the the free and forced vibration of systems analyzed to determine the effects of vibration isolation through the belts. The analytical results of the mathematical model for a belt-driven system are listed as follows.

(1) The two-dimensional mathematical model of support springs by pulleys for a belt-driven system have been presented, and the four non-linear governing equations of motion and twelve non-linear boundary conditions were derived.

(2) The perburbation method was applied to the derived equations and then linearized. The discretization procedure using Galerkin's weak forms was performed, in order to complete the equations of motion of a belt-driven system.

TABLE 7
Results of dynamic analysis I(μm)

	Timing belt		Poly-flex belt	
Calculated position	x	z	x	z
Left pulley	2·013	2·16	−16·36	−0·1575
Right pulley	−0·03535	−2·16	−0·8805	0·1575

TABLE 8
Results of dynamic analysis II (μm)

	F_{eq} (N)					
	1·0		5·0		10·0	
Calculated position	x	z	x	z	x	z
Left pulley	−7·965	−0·195	−39·83	−0·975	−79·65	−1·95
Right pulley	−0·68	0·195	−3·406	0·975	−6·811	1·95

(3) In order to calculate the supporting stiffness of pulleys, the bearing stiffness to support the motor spindle was used in the driving part, and the bearing stiffness to support the main spindle was used in the driven part. From the non-linear relation between the equivalent stiffness and the load applied to the bearing, a program was developed to calculate the equivalent stiffness for the loads applied to the bearings.

(4) By using the derived governing equations and boundary conditions, the free vibration analyses of an actual belt-driven system was performed. From the

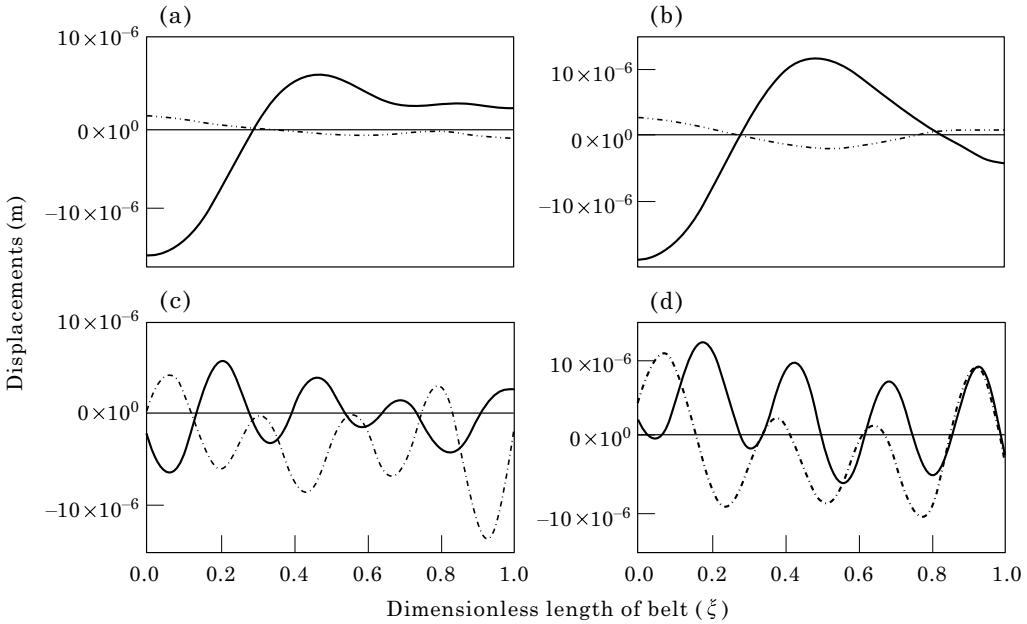

Figure 6. Dynamic displacements of the poly-flex belt (—) and the timing belt (- - -): (a) $\bar{u}$ of the primary belt; (b) u of the secondary belt; (c) $\bar{w}$ of the primary belt; (d) w of the secondary belt. The properties of the belt and the support stiffnesses are listed in Tables 1 and 2. Table 6 contains other relevant data.

results of these analyses, the natural frequencies and modes of system were obtained, confirming the couplings between the belt and the boundary conditions through the fact that each pair of the natural frequencies came out as shown in Tables 3–5. These phenomena were a result of considering the effects of the boundary conditions, namely, the longitudinal displacements, and the transverse displacements that characterize the pulley rotation and translation in each mode. It is clear that the longitudinal motions and the transverse motions oscillate the pulleys, and thus couple the motions of the belts as reported in Mote's [9] study.

(5) Free vibration analyses were performed for varying belt lengths, belt tensions, belt elastic moduli, belt velocities and pulley masses, confirming that the main parameters affecting the natural frequencies of the system were the length, the tension and the elastic modulus.

(6) Forced vibration analyses were performed for two belt types, and from the results of these analyses, one found that the effects of vibrational isolation of a poly-flex belt were larger than those of a timing belt.

REFERENCES

1. F. R. Archibald and A. G. Emslie 1956 *Journal of Applied Mechanics* **25**, 347–348. The vibration of a string having a uniform motion along its length.
2. C. D. Mote, Jr. 1966 *Transactions of the American Society of Mechanical Engineers*, *Journal of Applied Mechanics* **33**, 463–464. On the nonlinear oscillation of an axially moving strings.
3. M. A. Moustafa and F. K. Salman 1976 *Transactions of the American Society of Mechanical Engineers*, *Journal of Engineering for Industry* **98**, 869–875. Dynamic properties of a moving thread line.
4. S. Naguleswaran and J. H. Williams 1968 *International Journal of Mechanical Science* **10**, 239–250. Lateral vibration of band-saw blades, pulley belts and the like.
5. A. Simpson 1973 *Journal of Mechanical Engineering Science* **15**, 159–164. Transverse modes and frequencies of beams translating between fixed end supports.
6. A. G. Ulsoy and C. D. Mote, Jr. 1982 *Transactions of the American Society of Mechanical Engineers*, *Journal of Engineering for Industry* **104**, 71–77. Vibration of wide band saw blades.
7. Y. S. Chung, J. S. Chae and S. InDong 1982 *Journal of Korean Society of Mechanical Engineers* **6**, 93–99. A study on the vibration characteristics of V-belt driven system.
8. K. W. Wang and C. D. Mote, Jr. 1986 *Journal of Sound and Vibration* **109**, 237–258. Vibration coupling analysis of band/wheel mechanical systems.
9. C. D. Mote, Jr. and W. Z. Wu 1985 *Journal of Sound and Vibration* **102**, 1–9. Vibration coupling in continuous belt and band systems.
10. S. K. Kim 1988 *Master Thesis of Seoul National University*. A study on the analysis of dynamic characteristics of a main spindle considering nonlinearity of bearing.
11. A. H. Nahfeh and D. T. Mook 1979 *Nonlinear Oscillations*. New York: John Wiley.
12. L. Meirovitch 1967 *Analytical Methods in Vibrations*. New York: Macmillan.
13. S. K. Kim 1994 *Ph.D Thesis*, *Seoul National University*. A study on the vibration characteristics of a driven system with belt and magnetic coupling.

APPENDIX

A1. *Expansion of* $\delta H = \int_{t_1}^{t_2} (\delta T - \delta U + \delta W)\, \mathrm{d}t$ (11)

$$
\begin{aligned}
\delta H = \int_{t_1}^{t_2} \Bigg[\int_0^L [& \{-m\hat{u}_{,tt} + (EA - mc^2)\hat{u}_{,xx} - 2mc\hat{u}_{,xt} + EA\hat{w}_{,x}\hat{w}_{,xx}\}\ \delta\hat{u} \\
& + \{-m\hat{\bar{u}}_{,tt} + (EA - mc^2)\hat{\bar{u}}_{,xx} + 2mc\hat{\bar{u}}_{,xt} + EA\hat{\bar{w}}_{,x}\hat{\bar{w}}_{,xx}\}\ \delta\hat{\bar{u}} \\
& + \{-m\hat{w}_{,tt} + EA(\hat{u}_{,xx}\hat{w}_{,x}\hat{u}_{,x}\hat{w}_{,xx}) + 1{\cdot}5EA\hat{w}_{,x}^2\hat{w}_{,xx} - EI\hat{w}_{,xxxx} \\
& + (R - mc^2)\hat{w}_{,xx} - 2mc\hat{w}_{,xt}\}\ \delta\hat{w} \\
& + \{-m\hat{\bar{w}}_{,tt} + EA(\hat{\bar{u}}_{,xx}\hat{\bar{w}}_{,x} + \hat{\bar{u}}_{,x}\hat{\bar{w}}_{,xx}) \\
& + 1{\cdot}5EA\hat{\bar{w}}_{,x}^2\hat{\bar{w}}_{,xx} - EI\hat{\bar{w}}_{,xxxx} + (R - mc^2)\hat{\bar{w}}_{,xx} + 2mc\hat{\bar{w}}_{,xt}\}\ \delta\hat{\bar{w}} \Bigg]\, \mathrm{d}x \\
& + \{-EA\hat{u}_{,x}(L,t) - (EA/2)\hat{w}_{,x}^2(L,t) - (\hat{J}_R/4r_R^2)(\hat{u}_{,tt}(L,t) - \hat{\bar{u}}_{,tt}(L,t)) \\
& - (\hat{M}_R/4)(\hat{u}_{,tt}(L,t) + \hat{\bar{u}}_{,tt}(L,t)) - (\hat{k}_{Rx}/4)(\hat{u}_{,tt}(L,t) + \hat{\bar{u}}_{,tt}(L,t))\}\ \delta\hat{u}(L,t) \\
& - \{-EA\hat{u}_{,x}(0,t) - (EA/2)\hat{w}_{,x}^2(0,t) + (\hat{J}_L/4r_L^2)(\hat{u}_{,tt}(0,t) - \hat{\bar{u}}_{,tt}(0,t)) \\
& + (\hat{M}_L/4)(\hat{u}_{,tt}(0,t) + \hat{\bar{u}}_{,tt}(0,t)) \\
& + (\hat{k}_{Lx}/4)(\hat{u}_{,tt}(0,t) + \hat{\bar{u}}_{,tt}(0,t)) - f_x/2\}\ \delta\hat{u}(0,t) \\
& + \{-EA\hat{\bar{u}}_{,x}(L,t) - (EA/2)\hat{\bar{w}}_{,x}^2(L,t) + (\hat{J}_R/4r_R^2)(\hat{u}_{,tt}(L,t) - \hat{\bar{u}}_{,tt}(L,t)) \\
& - (\hat{M}_R/4)(\hat{u}_{,tt}(L,t) + \hat{\bar{u}}_{,tt}(L,t)) - (\hat{k}_{Rx}/4)(\hat{u}_{,tt}(L,t) + \hat{\bar{u}}_{,tt}(L,t))\}\ \delta\hat{\bar{u}}(L,t) \\
& - \{-EA\hat{\bar{u}}_{,x}(0,t) - (EA/2)\hat{\bar{w}}_{,x}^2(0,t) - (\hat{J}_L/4r_L^2)(\hat{u}_{,tt}(0,t) - \hat{\bar{u}}_{,tt}(0,t)) \\
& + (\hat{M}_L/4)(\hat{u}_{,tt}(0,t) + \hat{\bar{u}}_{,tt}(0,t)) \\
& + (\hat{k}_{Lx}/4)(\hat{u}_{,tt}(0,t) + \hat{\bar{u}}_{,tt}(0,t)) - f_x/2\}\ \delta\hat{\bar{u}}(0,t) \\
& + \{-EA\hat{u}_{,x}(L,t)\hat{w}_{,x}(L,t) - (EA/2)\hat{w}_{,x}^3(L,t) + EI\hat{w}_{,xxx}(L,t) - R\hat{w}_{,x}(L,t) \\
& - (\hat{M}_R/4)(\hat{w}_{,xx}(L,t) + \hat{\bar{w}}_{,xx}(L,t)) - (\hat{k}_{Ry}/4)(\hat{w}_{,xx}(L,t) + \hat{\bar{w}}_{,xx}(L,t))\}\ \delta\hat{w}(L,t) \\
& - \{-EA\hat{u}_{,x}(0,t)\hat{w}_{,x}(0,t) - (EA/2)\hat{w}_{,x}^3(0,t) + EI\hat{w}_{,xxx}(0,t) - R\hat{w}_{,x}(0,t) \\
& + (\hat{M}_L/4)(\hat{w}_{,xx}(0,t) + \hat{\bar{w}}_{,xx}(0,t)) + (\hat{k}_{Ly}/4)(\hat{w}_{,xx}(0,t) + \hat{\bar{w}}_{,xx}(0,t))\}\ \delta\hat{w}(0,t) \\
& + \{-EA\hat{\bar{u}}_{,x}(L,t)\hat{\bar{w}}_{,x}(L,t) - (EA/2)\hat{\bar{w}}_{,x}^3(L,t) + EI\hat{\bar{w}}_{,xxx}(L,t) - R\hat{\bar{w}}_{,x}(L,t)
\end{aligned}
$$

$$- (\hat{M}_L/4)(\hat{w}_{,xx}(L, t) + \hat{\bar{w}}_{,xx}(L, t)) - (\hat{k}_{Ly}/4)(\hat{w}_{,xx}(L, t) + \hat{\bar{w}}_{,xx}(L, t))\} \, \delta\hat{\bar{w}}(L, t)$$

$$- \{-EA\hat{\bar{u}}_{,x}(0, t)\hat{\bar{w}}_{,x}(0, t) - (EA/2)\hat{\bar{w}}^3_{,x}(0, t) + EI\hat{\bar{w}}_{,xxx}(0, t) - R\hat{\bar{w}}_{,x}(0, t)$$

$$+ (\hat{M}_L/4)(\hat{w}_{,xx}(0, t) + \hat{\bar{w}}_{,xx}(0, t))$$

$$+ (\hat{k}_{Ly}/4)(\hat{w}_{,xx}(0, t) + \hat{\bar{w}}_{,xx}(0, t)) - f_y/2\} \, \delta\hat{\bar{w}}(0, t)$$

$$- \{\hat{M}\hat{M}_L - EI\hat{w}_{,xx}(0, t)\} \, \delta\hat{w}_{,x}(0, t) + \{\hat{M}\hat{M}_R - EI\hat{w}_{,xx}(L, t)\} \, \delta\hat{w}_{,x}(L, t)$$

$$+ \{\hat{M}\hat{M}_L + EI\hat{\bar{w}}_{,xx}(0, t)\} \, \delta\hat{\bar{w}}_{,x}(0, t) + \{\hat{M}\hat{M}_R - EI\hat{\bar{w}}_{,xx}(L, t)\} \, \delta\hat{\bar{w}}_{,x}(L, t)] = 0.$$

By inserting Equation (26) *into the equations* (12)–(25) *to eliminate the nonlinear terms, four linear governing equations and twelve boundary conditions are derived.*

$$u(\xi, \tau) = u^*(\xi) + u(\xi, \tau), \quad \bar{u}(\xi, \tau) = \bar{u}^*(\xi) + \bar{u}(\xi, \tau),$$

$$w(\xi, \tau) = w^*(\xi) + w(\xi, \tau), \quad \bar{w}(\xi, \tau) = \bar{w}^*(\xi) + \bar{w}(\xi, \tau),$$

Governing equation

$$\ddot{u} + 2s\dot{u}' = \Phi u'' - \gamma(w^{*\prime}w')' = 0, \quad \ddot{\bar{\mathbf{u}}} - 2s\ddot{\bar{\mathbf{u}}}' - \Phi\bar{u}'' - \gamma(\bar{w}^{*\prime}\bar{w}')' = 0,$$

$$\ddot{w} + 2s\dot{w}' - \Psi w'' + w'''' - \gamma(w^{*\prime}u' + u^{*\prime}w'), \quad - 1{\cdot}5\alpha(w^{*2}w'' + 2w^{*\prime}w^{*\prime\prime}w') = 0,$$

$$\ddot{\bar{\mathbf{w}}} - 2s\ddot{\bar{\mathbf{w}}}' - \Psi\bar{w}'' + \bar{w}'''' - \gamma(\bar{w}^{*\prime}\bar{u}' + \bar{u}^{*\prime}\bar{w}'), \quad - 1{\cdot}5\alpha(\bar{w}^{*\prime 2}\bar{w}'' + 2\bar{w}^{*\prime}\bar{w}^{*\prime\prime}\bar{w}') = 0.$$

Boundary conditions

$$(J_L/2\rho_L^2)(\ddot{u}(0, t) - \ddot{\bar{\mathbf{u}}}(0, \tau)) - \beta(u'(0, \tau) - \bar{u}'(0, \tau)) - \gamma(w^{*\prime}(0)w'(0, \tau) - \bar{w}^{*\prime}(0)\bar{w}'(0, \tau)) = 0,$$

$$(M_L/2)(\ddot{u}(0, t) + \ddot{\bar{\mathbf{u}}}(0, \tau)) + (k_{Lx}/2)(u(0, \tau) + \bar{u}(0, \tau)) - \beta(u'(0, \tau) + \bar{u}'(0, \tau)) - \gamma(w^{*\prime}(0)w'(0, \tau) + \bar{w}^{*\prime}(0)\bar{w}'(0, \tau)) = \bar{f}_x,$$

$$(J_R/2\rho_R^2)(\ddot{u}(1, \tau) - \ddot{\bar{\mathbf{u}}}(1, \tau)) + \beta(u'(1, \tau) - \bar{u}'(1, \tau)) + \gamma(w^{*\prime}(1)w'(1, \tau) + \bar{w}^{*\prime}(1)\bar{w}'(1, \tau)) = 0,$$

$$(M_R/2)(\ddot{u}(1, t) + \ddot{\bar{\mathbf{u}}}(1, \tau)) + (k_{Rx}/2)(u(1, \tau) + \bar{u}(1, \tau)) + \beta(u'(1, \tau) + \bar{u}'(1, \tau)) + \gamma(w^{*\prime}(1)w'(1, \tau) + \bar{w}^{*\prime}(1)\bar{w}'(1, \tau)) = 0,$$

$$(w'''(0,\tau)-\bar{w}'''(0,\tau))-R_n(w'(0,\tau)-\bar{w}'(0,\tau))$$
$$-\tfrac{3}{2}\alpha(w^{*\prime 2}(0)w'(0,\tau)-\bar{w}^{*\prime 2}(0)\bar{w}'(0,\tau))$$
$$-\gamma(u^{*\prime}(0)w'(0,\tau)+w^{*\prime}(0)u'(0,\tau)-\bar{u}^{*\prime}(0)\bar{w}'(0,\tau)-\bar{w}^{*\prime}(0)\bar{u}'(0,\tau))=0$$

$$(M_L/2)(\ddot{w}(0,t)+\ddot{\bar{\mathbf{w}}}(0,\tau))+(k_{Lx}/2)(w(0,\tau)+\bar{w}(0,\tau))$$
$$+(w'''(0,\tau)+\bar{w}'''(0,\tau))-R_n(w'(0,\tau)+\bar{w}'(0,\tau))$$
$$-\tfrac{3}{2}\alpha(w^{*\prime 2}(0)w'(0,\tau)+\bar{w}^{*\prime 2}(0)\bar{w}'(0,\tau))$$
$$-\gamma(u^{*\prime}(0)w'(0,\tau)+w^{*\prime}(0)u'(0,\tau)$$
$$+\bar{u}^{*\prime}(0)\bar{w}'(0,\tau)+\bar{w}^{*\prime}(0)\bar{u}'(0,\tau))=\bar{f}_z,$$

$$(w'''(1,\tau)-\bar{w}'''(1,\tau))-R_n(w'(1,\tau)-\bar{w}'(1,\tau))$$
$$-\tfrac{3}{2}\alpha(w^{*\prime 2}(1)w'(1,\tau)-\bar{w}^{*\prime 2}(1)\bar{w}'(1,\tau))$$
$$-\gamma(u^{*\prime}(1)w'(1,\tau)+w^{*\prime}(1)u'(1,\tau)-\bar{u}^{*\prime}(1)\bar{w}'(1,\tau)-\bar{w}^{*\prime}(1)\bar{u}(1,\tau))=0,$$

$$(M_R/2)(\ddot{w}(1,\tau)+\ddot{\bar{\mathbf{w}}}(1,\tau))+(k_{Rz}/2)(w(1,\tau)+\bar{w}(1,\tau))$$
$$-(w'''(1,\tau)+\bar{w}'''(1,\tau))+R_n(w'(1,\tau)+\bar{w}'(1,\tau))$$
$$-\tfrac{3}{2}\alpha(w^{*\prime 2}(1)w'(1,\tau)+\bar{w}^{*\prime 2}(1)\bar{w}'(1,\tau))$$
$$+\gamma(u^{*\prime}(1)w'(1,\tau)+w^{*\prime}(1)u'(1,\tau)$$
$$+\bar{u}^{*\prime}(1)\bar{w}'(1,\tau)+\bar{w}^{*\prime}(1)\bar{u}'(1,\tau))=0,$$

$$w''(0,\tau)=\bar{w}''(0,\tau)=0,\quad w''(1,\tau)=\bar{w}''(1,\tau)=0.$$